Available online at www.sciencedirect.com
SCIENCE DIRECT®
Journal of Sound and Vibration 275 (2004) 591–603
JOURNAL OF SOUND AND VIBRATION
www.elsevier.com/locate/jsvi

Dynamics of a dry friction oscillator under two-frequency excitations

G. Cheng, J.W. Zu*

Department of Mechanical & Industrial Engineering, University of Toronto, 5 King's College Road, Toronto, Ontario, Canada M5S 3G8

Received 28 January 2003; accepted 26 June 2003

Abstract

In this paper, the dynamic behavior of a dry friction oscillator subjected to simultaneous self and external excitations is studied. The dry friction in the system follows the classical Coulomb's law, and the external excitation consists of two harmonic forces with different frequencies. The focus of the paper is laid on bifurcation analysis to gain insight into the influence of the two-frequency excitation upon the qualitative features of system dynamics. Numerical simulations are performed and the simulation results are visualized by means of bifurcation diagrams, Poincaré sections and Lyapunov exponents. New and interesting conclusions are reached from the study. It is shown that small excitation frequencies and amplitudes tend to cause chaos in the system, whereas large excitation amplitudes can induce only periodic motions. Furthermore, it is found that the probability of the occurrence of periodic motions increases, as the ratio between the two excitation frequencies increases.

1. Introduction

The vibration of dry friction damped systems has been actively studied for many years, not only because dry friction appears frequently in everyday life as well as in engineering systems, but also because it poses challenges to researchers as a discontinuous non-linearity. Really complex dynamics, e.g. chaos, can be exhibited from dry friction damped systems even in its simplest form, Coulomb damping.

Among the earliest research on dry friction oscillators is that of Den Hartog [1], where an exact solution was found for the steady state vibration of an SDOF harmonically excited system with

*Corresponding author. Tel.: +1-416-978-0961; fax: +1-416-978-7753.
E-mail address: zu@mie.utoronto.ca (J.W. Zu).

0022-460X/$ - see front matter
doi:10.1016/j.jsv.2003.06.027

dry friction. He also performed several experimental tests to verify his solutions. Since then, much work has been done in this field. Pierre et al. [2] presented a multi-harmonic frequency domain analysis of Coulomb damped systems with one and two d.o.f., using an incremental harmonic balance method. Later, Feeny and Moon [3] investigated the geometry of chaotic attractors for dry friction oscillators experimentally and numerically. In their study, three friction laws were examined. In Mueller's paper [4], an analytical method of calculating Lyapunov exponents for non-linear dynamic systems with discontinuity was proposed and was applied to the analysis of a Coulomb damped oscillator. Oestreich et al. [5] employed a one-dimensional map to discuss bifurcation and stability of a non-smooth friction oscillator on a moving base, and the map approach was shown to be an efficient and illustrative way to carry out such analysis. The response of a dry friction oscillator on a moving base was also analyzed by Andreaus and Casini [6], with emphasis laid on the influence of the base speed and the friction modelling on the system response. Using a smoothing procedure, Van De Vrande et al. [7] computed both stable and unstable periodic solutions for the stick-slip vibration of an autonomous system with dry friction. More recently, the work of Galvanetto [8,9] dealt with discontinuous bifurcations in a two-block system affected by dry friction, as well as numerical techniques to compute the Lyapunov exponents of discontinuous maps implicitly defined.

In all of the research above, either no excitation or only a single harmonic excitation was assumed. In practice, however, multi-excitations can exist in various vibration systems with dry friction, and they may have a dramatic effect on the system's dynamic characteristics. To address the lack of research on this issue, the authors [10] studied the vibration of a dry friction oscillator subjected to two harmonic disturbing forces with different frequencies and determined periodic solutions for both non-stick and stick-slip motions. In this paper, we further our study into the chaotic aspects of two-frequency oscillations with dry friction. The dynamics of a Coulomb friction oscillator subjected to two harmonic excitations on a moving belt with constant velocity is investigated, with focus laid on bifurcation analysis to illustrate the influence of the two-frequency excitation upon the system behavior. It is found that small excitation frequencies and amplitudes tend to yield chaotic motions. Furthermore, as the ratio between the two excitation frequencies increases, less likely chaotic motions will occur.

2. System description

The system under investigation is shown in Fig. 1, where a mass m is connected to a fixed support via a linear spring with stiffness k and a viscous damper with damping coefficient c, and is sliding on a moving belt with constant velocity v_0. The mass is subjected to two harmonic excitations with the same amplitude P but different frequencies ω_1 and ω_2. In addition, dry friction can occur between the mass and the belt. In the study, the following assumptions are made:

1. The two excitation frequencies are proportional to each other in such a way that

$$\frac{\omega_2}{\omega_1} \equiv v = \frac{M}{N}, \tag{1}$$

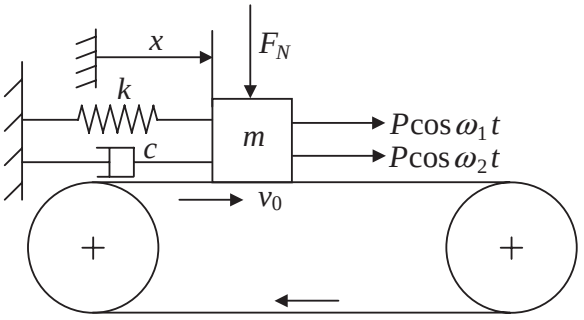

Fig. 1. Model of a dry friction oscillator.

where M and N are incommensurable integers (If $M/N = 1$, the case degenerates to the single excitation case).

2. The dry friction between the mass and the belt follows Coulomb's friction law characterized by a static friction coefficient μ_s and a smaller kinetic friction coefficient μ_k.

The equation of motion for the oscillator is given by

$$m\ddot{x} + c\dot{x} + kx = -\mu F_N \operatorname{sgn}(\dot{x} - v_0) + P\cos\omega_1 t + P\cos\omega_2 t, \tag{2}$$

where x denotes the displacement of the mass, F_N is the normal force in the contact area, and

$$\mu = \begin{cases} \mu_k & (\dot{x} \neq v_0), \\ \mu_s & (\dot{x} = v_0), \end{cases} \quad \operatorname{sgn}(y) \begin{cases} = 1 & (y > 0), \\ \in [-1, 1] & (y = 0), y \in \mathbf{R}, \\ = -1 & (y < 0). \end{cases} \tag{3,4}$$

By defining the quantities

$$\omega_0 = \sqrt{\frac{k}{m}}, \quad \tau = \omega_0 t, \quad \lambda = \frac{c}{m\omega_0}, \quad u_0 = \frac{P}{m\omega_0^2}, \quad x_v = \frac{v_0}{\omega_0},$$
$$x_f = \frac{\mu F_N}{k} = \begin{cases} x_{fk} & (\dot{x} \neq v_0) \\ x_{fs} & (\dot{x} = v_0), \end{cases} \quad \eta = \frac{\omega_1}{\omega_0}, \tag{5}$$

Eq. (2) can be normalized as

$$x'' + \lambda x' + x = -x_f \operatorname{sgn}(x' - x_v) + u_0 \cos(\eta\tau) + u_0 \cos(v\eta\tau) \tag{6}$$

in which the prime indicates differentiation with respect to the non-dimensional time τ.

3. Dynamic analysis

3.1. Solutions for slip and stick modes

Since Eq. (6) is piecewise linear, an analytical solution can be formulated for the slip mode ($x' \neq x_v$) and the stick mode ($x' = x_v$), respectively, with the initial conditions

$$x(\tau_0) = x_0, \quad x'(\tau_0) = x_0'. \tag{7}$$

For the slip mode, the solution is obtained:

$$x(\tau) = \mp x_{fk} + e^{-\lambda(\tau-\tau_0)/2}[C_1 \cos p(\tau-\tau_0) + C_2 \sin p(\tau-\tau_0)] + u_0\beta_1 \cos(\eta\tau - \theta_1) + u_0\beta_2 \cos(v\eta\tau - \theta_2), \tag{8}$$

where

$$C_1 = x_0 \pm x_{fk} - u_0\beta_1 \cos(\eta\tau_0 - \theta_1) - u_0\beta_2 \cos(v\eta\tau_0 - \theta_2), \tag{9}$$

$$C_2 = \frac{1}{p}\left[x_0' + \frac{\lambda}{2}C_1 + u_0\beta_1\eta \sin(\eta\tau_0 - \theta_1) + u_0\beta_2 v\eta \sin(v\eta\tau_0 - \theta_2)\right], \tag{10}$$

$$p = \sqrt{1-\lambda^2/4}, \quad \beta_1 = 1/\sqrt{(1-\eta^2)^2 + \lambda^2\eta^2}, \quad \beta_2 = 1/\sqrt{(1-v^2\eta^2)^2 + \lambda^2 v^2\eta^2},$$
$$\theta_1 = \tan^{-1}\frac{\lambda\eta}{1-\eta^2}, \quad \theta_2 = \tan^{-1}\frac{\lambda v\eta}{1-v^2\eta^2}. \tag{11}$$

It is noted that the upper and lower part of the compound signs $\mp$ and $\pm$ in Eqs. (8) and (9) corresponds to the case of $x' > x_v$ and of $x' < x_v$, respectively. For the stick mode, the solution simply becomes

$$x(\tau) = x_0 + x_v(\tau - \tau_0). \tag{12}$$

The final state of one mode is implemented as the initial state of the other. The state of transition from the slip mode to the stick mode and vice versa is determined by the following equations, respectively:

$$x_v = e^{-\lambda\tau/2}p(-C_1 \sin p\tau + C_2 \cos p\tau) - \frac{\lambda}{2}e^{-\lambda\tau/2}(C_1 \cos p\tau + C_2 \sin p\tau) - u_0\beta_1\eta \sin[\eta(\tau+\tau_0) - \theta_1] - u_0\beta_2 v\eta \sin[v\eta(\tau+\tau_0) - \theta_2], \tag{13}$$

$$|-\lambda x_v - x_0 - x_v(\tau - \tau_0) + u_0 \cos(\eta\tau) + u_0 \cos(v\eta\tau)| = x_{fs}. \tag{14}$$

Since the above two equations are transcendental and an explicit solution for τ is impossible, a numerical procedure is needed to solve τ.

3.2. Phase space and Poincaré section

The two external harmonic excitations on the system can be regarded as one non-harmonic, yet periodic excitation whose circular frequency is calculated as

$$\omega = \frac{\eta}{N}. \tag{15}$$

Thus, it is possible to construct a three-dimensional phase space to study the dynamics of the system. By introducing

$$\varphi \equiv \omega\tau \bmod 2\pi \in [0, 2\pi) \tag{16}$$

we define a phase space in cylindrical co-ordinates (r, θ, z) as

$$r = x, \quad \theta = \varphi, \quad z = x'. \tag{17}$$

In the above phase space, two-dimensional Poincaré sections can also be defined:

$$\{(x, x')|\varphi = \varphi_0 \in [0, 2\pi)\}, \tag{18}$$

where φ_0 is an arbitrary real constant.

3.3. One-point map and Lyapunov exponents

One efficient way to study dry friction oscillators is to introduce maps between different points in the state space so that the dimension of the system is reduced. Naturally, one can choose stick-to-slip or slip-to-stick transition states as mapping points as they correspond to the discontinuity of dry friction. In this study, the stick-to-slip transition states are considered. Let x_n be the nth stick-to-slip position of the mass and φ_n be its corresponding phase angle, as defined in Eq. (16). The following relationship between x_n and φ_n can be derived

$$x_n = -\lambda x_v \mp x_{fs} + u_0 \cos(N\varphi_n) + u_0 \cos(M\varphi_n), \tag{19}$$

in which the upper and lower part of the compound sign $\mp$ corresponds to the entered slip mode where $x' > x_v$ and $x' < x_v$, respectively. With x_n, bifurcation analysis can be carried out to study the influence of bifurcation parameters on the system dynamics. Based on φ_n, the following one-point map is introduced, which was originally proposed in Ref. [5] for the single-excitation case:

$$H : \varphi_n \mapsto H(\varphi_n) = \varphi_{n+1} \quad (n = 1, 2, \ldots). \tag{20}$$

The above one-dimensional map allows a simple determination of the Lyapunov exponent Λ of the system, cf. Ref. [11]:

$$\Lambda = \lim_{n \to \infty} \frac{1}{n} \sum_{p=0}^{n-1} \ln|H'(\varphi_p)|. \tag{21}$$

It should be pointed out that with the system reduced to a one-dimensional map H, two Lyapunov exponents are lost. One of them is zero corresponding to a tangential perturbation direction, and the other equals minus infinity due to the two-dimensionality in the stick mode.

3.4. Computational method

Since analytical solutions for both slip and stick modes of the system are available, the computation errors arise solely from the detection of discontinuity, i.e., slip-to-stick or stick-to-slip transition. Therefore, the computation of the precise time value when the discontinuity occurs is of crucial importance. In our approach, we evaluate appropriate switch functions to judge if a transition happens. Six different time steps are adopted to make sure that the value of the transition time is precise to the order 10^{-12}, and thereby the accuracy of the results is guaranteed. To illustrate this procedure, a flow diagram for the detection of slip-to-stick time is shown schematically in Fig. 2.

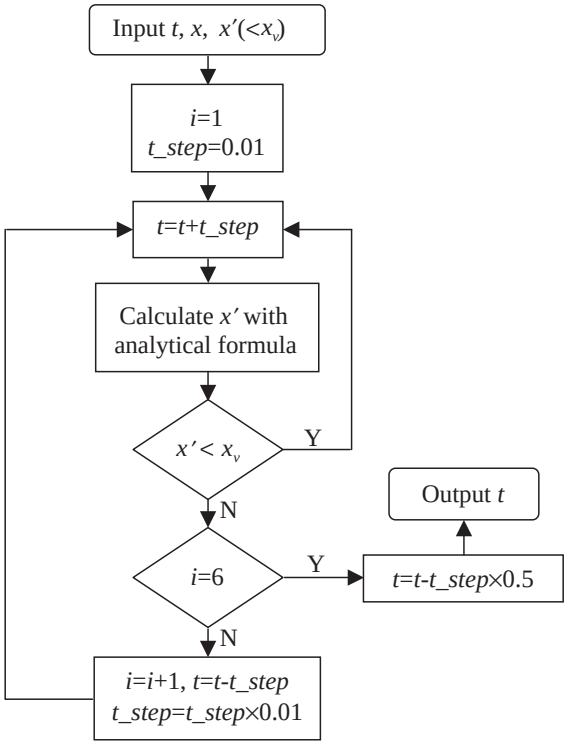

Fig. 2. Flow diagram for detecting slip-to-stick transition time.

4. Numerical results

The numerical study in this section concentrates on bifurcation analysis to illustrate the influence of the system's parameters on its dynamic behavior under various ratios between the two excitation frequencies, i.e., M/N. The bifurcation parameters adopted are: the ratio between frequencies ω_1 and ω_0, namely η, and the amplitude of the excitations, i.e., u_0. The basic system parameters, unless otherwise specified as bifurcation parameters, are assumed to take the values

$$\lambda = 0, \quad x_{fk} = 2.5, \quad x_{fs} = 4.0, \quad x_v = 1, \quad u_0 = 0.25, \quad \eta = \tfrac{2}{3}. \tag{22}$$

In what follows, numerical results are presented in two subsections corresponding to bifurcation parameters η and u_0, respectively.

4.1. Bifurcation analysis with η as parameter

In this subsection, bifurcation diagrams of the stick-to-slip transition displacement x are shown as a function of the parameter η, with different excitation frequency ratios, namely M/N. The figures reflect the steady motion of the mass since only post-transient points are plotted. Fig. 3(a) displays the case where $M=3$ and $N=5$. For η less than 0.75, the motion is basically chaotic. With larger values of η, one can distinguish multiple periodic solutions, of which the 3- and 5-period ones are distinct. From one of the chaos bands in Fig. 3(a) we choose the parameter

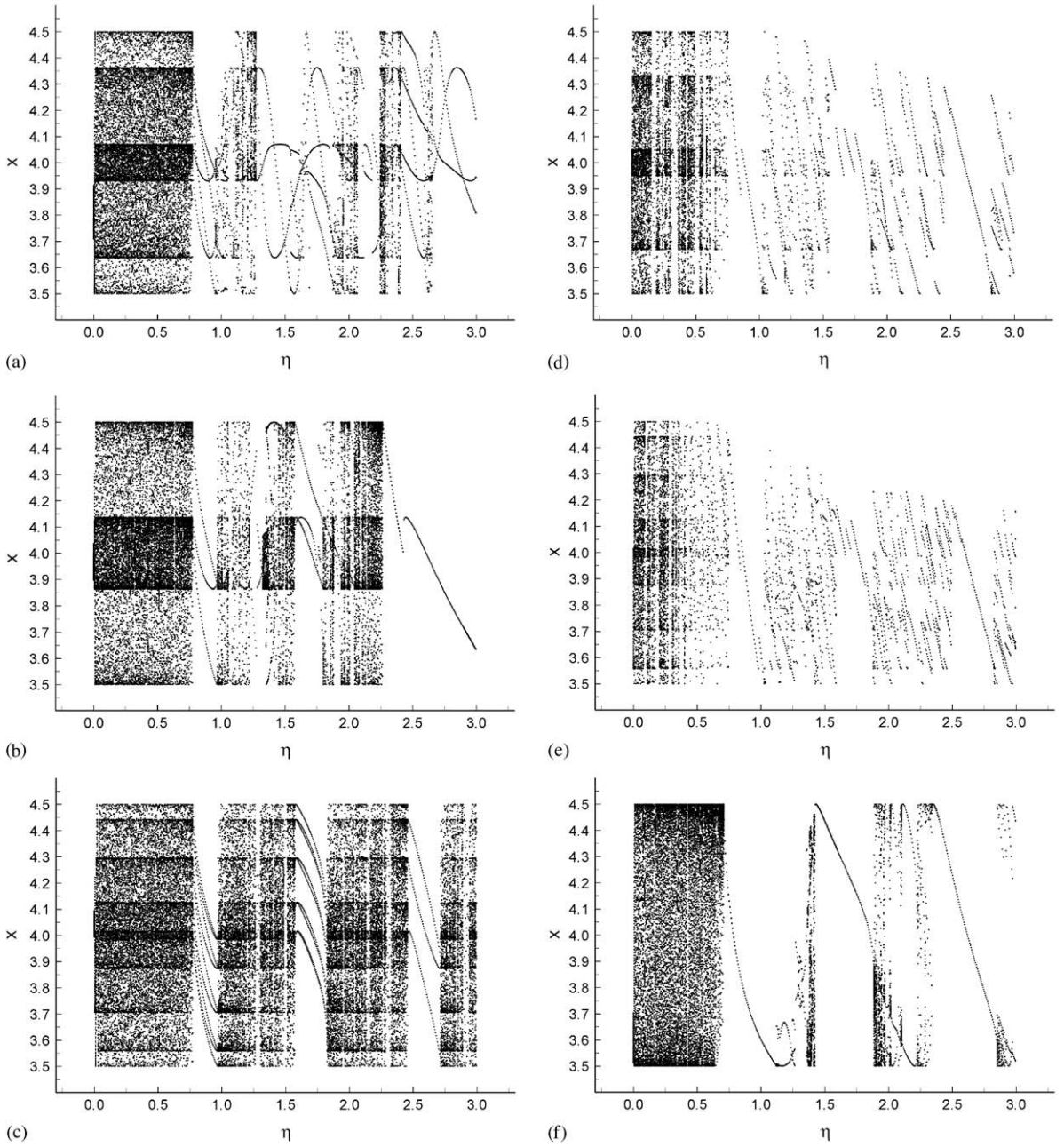

Fig. 3. Stick-to-slip displacement x vs. η: (a) $M = 3$, $N = 5$; (b) $M = 1$, $N = 3$; (c) $M = 1$, $N = 9$; (d) $M = 5$, $N = 1$; (e) $M = 9$, $N = 1$; (f) $M = 1$, $N = 1$.

$\eta = 2.304$ and examine its corresponding Poincaré section and Lyapunov exponent in Fig. 4. The Poincaré section ($\varphi = 0$) in Fig. 4(a) consists of line segments at irregular intervals, essentially dissimilar to the plot of finite points and of closed orbits which corresponds to periodic and

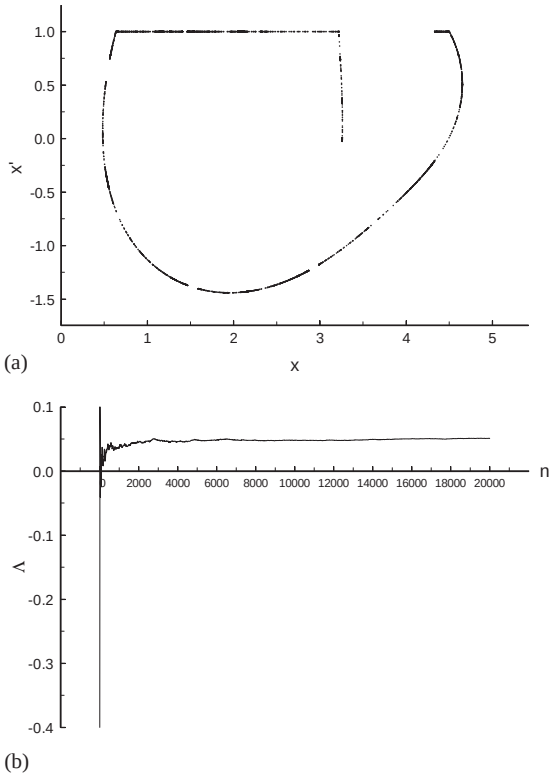

Fig. 4. (a) Poincaré section and (b) Lyapunov exponent with $M = 3$, $N = 5$ and $\eta = 2.304$.

quasiperiodic motions, respectively. Hence, the Poincaré section indicates chaos. In addition, the Lyapunov exponent converges to a positive number 0.051 along the increased number of iterates, as seen from Fig. 4(b). As well known, positive Lyapunov exponents are one defining characteristic of chaos. It is believed that the presence of chaos in the system is due to the difference between the static friction coefficient and the kinetic friction coefficient, since it was proven in Ref. [4] that chaos is impossible when the kinetic friction coefficient is equal to the static friction coefficient.

Fig. 3(b) illustrates the stick-to-slip transition displacement x versus η, where M and N are set to 1 and 3, respectively. A similar structure is demonstrated in comparison with Fig. 3(a): chaotic motions occupy the small η range while periodic windows appear with the increase of η. For this case, however, the obvious periodic solutions are of 1- and 3-period. A jump phenomenon in the 1-period solution is also noticed at $\eta = 2.43$. The enlargement of a narrow portion of Fig. 3(b), where $\eta \in [1.7975, 1.810]$, reveals the interesting phenomenon, see Fig. 5, that the periodic windows take on highly similar patterns. Particularly, the periodic window becomes narrower from right to left, with the periodic number increased by 3 consecutively.

Figs. 3(c)–(e) show the cases of M/N equal to $\frac{1}{9}$, $\frac{5}{1}$ and $\frac{9}{1}$, respectively. Apparently, all these plots comply with the aforementioned structure rule. Moreover, a trend in the influence of M/N on the system dynamic behavior is discovered from these figures together with the previous ones. It is

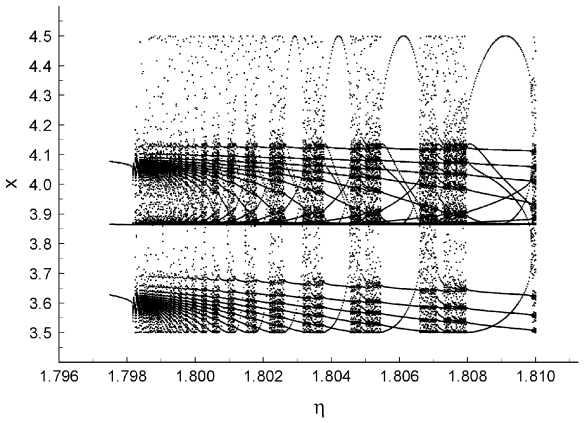

Fig. 5. Enlargement of part of Fig. 3(b) where η lies in [1.7975, 1.810].

observed that as M/N is increased from $\frac{1}{9}$ to $\frac{9}{1}$, less chaotic motions occur and more periodic motions take place, with respect to the parameter η.

With $M = N = 1$, the two-frequency excitation on the system becomes a single-frequency one. The numerical results for this special case are displayed in Fig. 3(f). As expected, the proportion of chaotic solutions of the system, according to the parameter η, lies between those for the cases of $M/N > 1$ and $M/N < 1$. In addition, the region with η lying between 1.955 and 1.980 of Fig. 3(f) is enlarged in Fig. 6(a), where a period-doubling route to chaos is manifested. The corresponding Lyapunov exponents are presented in Fig. 6(b), which, together with Figs. 3(f) and 6(a), shows a very good agreement with the results from Ref. [5], where the single-excitation case was studied.

4.2. *Bifurcation analysis with u_0 as parameter*

The numerical results for the system behavior depending on the excitation amplitude u_0 under various M/N are given in Figs. 7–9. Fig. 7(a) illustrates the stick-to-slip displacement x against u_0 with $M = 4$ and $N = 17$. It is shown that for small values of u_0 only chaotic solutions can be distinguished while for larger u_0 typical windows appear. This is similar to the previous situations with η as parameter. What's different, however, is that when u_0 becomes large enough, only periodic motions happen and the periodic number, 17 in this case, coincides with N. Another interesting phenomenon is found that in the range of small u_0 where chaos occurs, the upper and lower limit values of x seem to grow linearly with the increase of u_0. In Fig. 8, the chaotic solution at $u_0 = 0.6$ of Fig. 7(a) is identified with the aid of Poincaré section and Lyapunov exponent plots. Clearly, both the Poincaré section and the Lyapunov exponent imply chaos.

Figs. 7(b)–(d) correspond to the cases of M/N equal to $\frac{1}{9}$, $\frac{3}{1}$ and $\frac{9}{1}$, respectively. All these plots verify the characteristics mentioned above: (1) as u_0 increases from zero, chaotic motions appear first, followed by alternate occurrence of periodic motions and chaos, except for the case $M/N = \frac{9}{1}$ where periodic solutions exist for the full range of u_0; (2) when u_0 is large enough, only periodic solutions occur whose periodic number is determined by N; and (3) in the range of small u_0 where chaos occurs, the limit values of x are linear functions of u_0. Furthermore, comparing Figs. 7(a)–(d) leads to the conclusion that the bigger M/N is the larger percentage periodic motions take up the

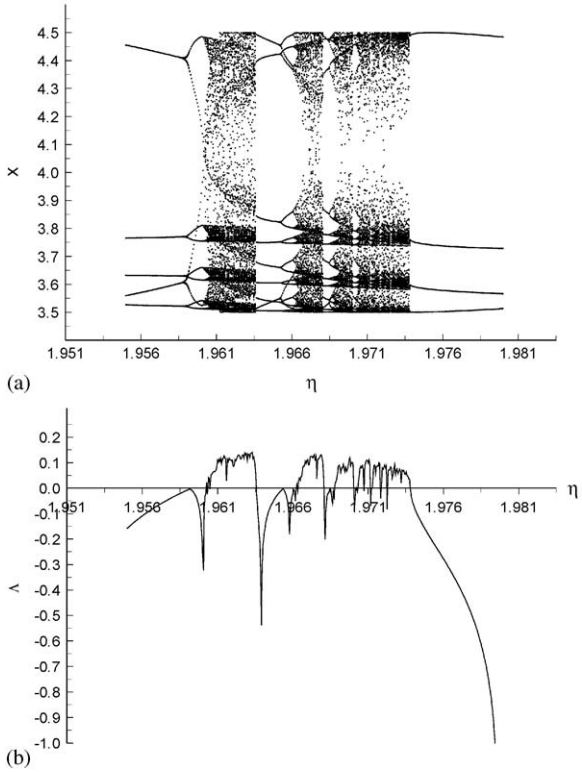

Fig. 6. (a) Enlargement of part of Fig. 3(f) and (b) the corresponding Lyapunov exponents.

scope of u_0. As a matter of fact, if M/N becomes big enough, such as $\frac{9}{1}$, only periodic solutions exist with respect to the parameter u_0.

The special case of $M = N = 1$ is plotted in Fig. 7(e), which obviously obeys all the aforementioned rules. The enlargement of one periodic window located at $u_0 \in [0.145, 0.152]$ demonstrates a unique pattern, as shown in Fig. 9.

5. Conclusions

The dynamic behavior of a Coulomb friction oscillator subjected to two-frequency excitations on a moving belt with constant velocity has been elaborated. The emphasis has been laid on bifurcation analysis to examine the influence of the system's parameters on its dynamics. Numerical simulations have been carried out and the simulation results suggest the following conclusions:

1. For both bifurcation parameters corresponding to the excitation amplitude and the excitation frequency, respectively, for small values only chaotic solutions can be distinguished, while for larger values periodic windows appear among chaos bands. Physically speaking, small excitation frequencies and amplitudes tend to yield chaotic motions.

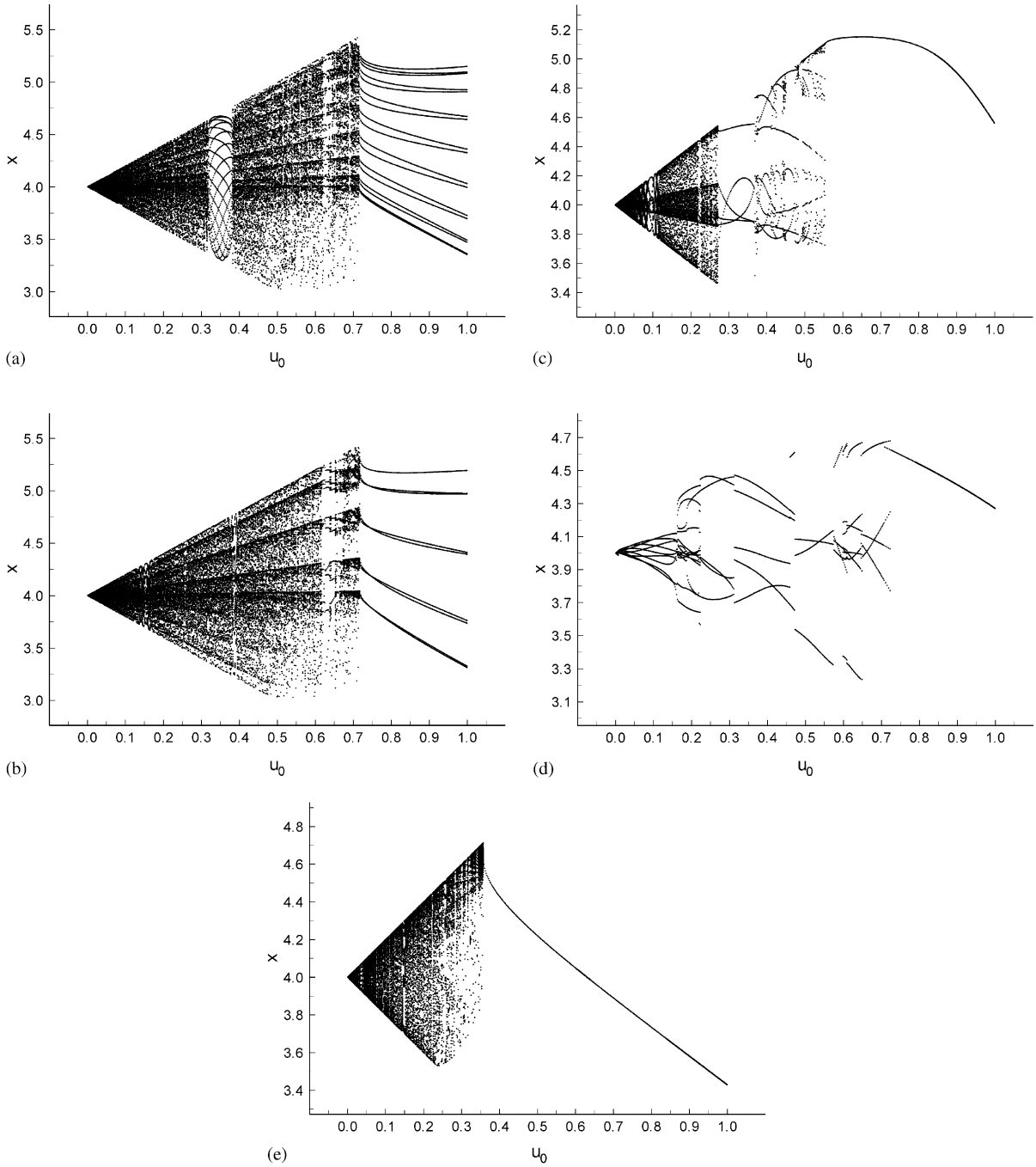

Fig. 7. Stick-to-slip displacement x vs. u_0: (a) $M = 4$, $N = 17$; (b) $M = 1$, $N = 9$; (c) $M = 3$, $N = 1$; (d) $M = 9$, $N = 1$; (e) $M = 1$, $N = 1$.

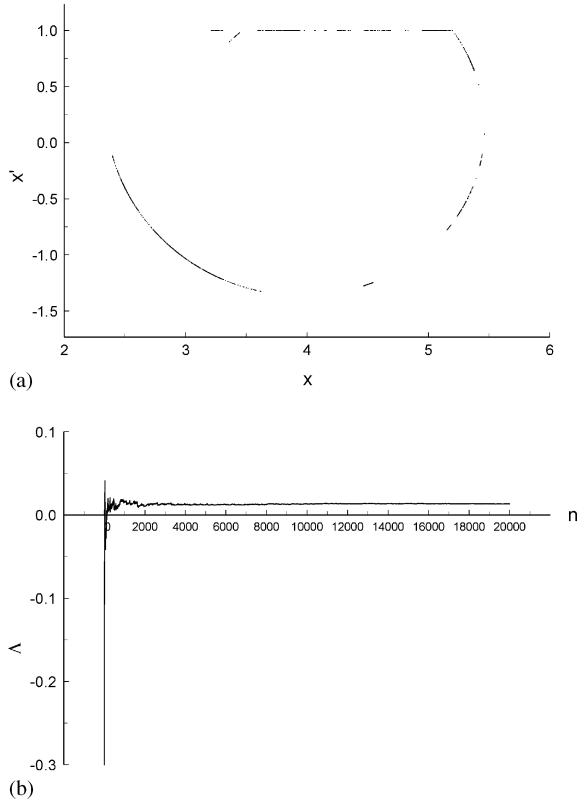

Fig. 8. (a) Poincaré section and (b) Lyapunov exponent with $M = 4$, $N = 17$ and $u_0 = 0.6$.

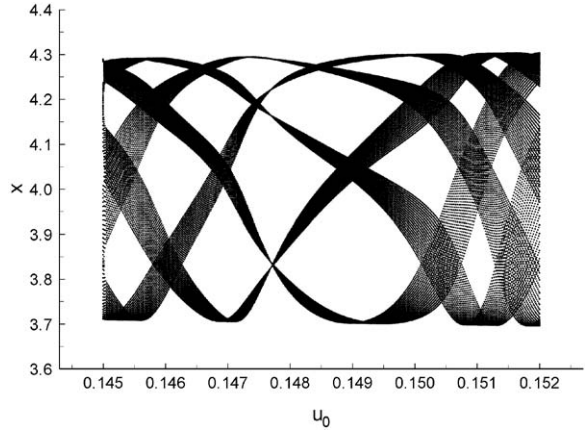

Fig. 9. Enlargement of part of Fig. 7(e) where u_0 lies in [0.145, 0.152].

2. For certain range of small excitation amplitudes where chaos occurs, the limit values of the stick-to-slip displacement depend linearly on the excitation amplitude. Moreover, as long as the excitation is sufficiently large, only periodic motion can happen, which

in turn leads to the conclusion that chaos can be caused by only relatively weak external excitations.

3. It is found that the ratio between the two excitation frequencies, namely M/N, has a significant impact upon the system dynamics. With respect to both bifurcation parameters, as M/N is increased, more likely periodic motions will occur than chaotic motions. In addition, when the excitation is large enough to induce only periodic solutions, the corresponding solutions are of N-period.

References

[1] J.P. Den Hartog, Forced vibrations with combined Coulomb and viscous friction, *Transactions of the American Society of Mechanical Engineers* 53 (1931) 107–115.
[2] C. Pierre, A.A. Ferri, E.H. Dowell, Multi-harmonic analysis of dry friction damped systems using an incremental harmonic balance method, *American Society of Mechanical Engineers, Journal of Applied Mechanics* 52 (1985) 958–964.
[3] B.F. Feeny, F.C. Moon, Chaos in a forced oscillator with dry friction: experiments and numerical modeling, *Journal of Sound and Vibration* 170 (1994) 303–323.
[4] P.C. Mueller, Calculation of Lyapunov exponents for dynamic systems with discontinuities, *Chaos, Solitons & Fractals* 5 (1995) 1671–1681.
[5] M. Oestreich, N. Hinrichs, K. Popp, Bifurcation and stability analysis for a non-smooth friction oscillator, *Archive of Applied Mechanics* 66 (1996) 301–314.
[6] U. Andreaus, P. Casini, Dynamics of friction oscillators excited by a moving base and/or driving force, *Journal of Sound and Vibration* 245 (2001) 685–699.
[7] B.L. Van De Vrande, D.H. Van Campen, A. De Kraker, An approximate analysis of dry-friction-induced stick-slip vibrations by a smoothing procedure, *Nonlinear Dynamics* 19 (1999) 157–169.
[8] U. Galvanetto, Some discontinuous bifurcations in a two-block stick-slip system, *Journal of Sound and Vibration* 248 (2001) 653–669.
[9] U. Galvanetto, Numerical computation of Lyapunov exponents in discontinuous maps implicitly defined, *Computer Physics Communications* 131 (2000) 1–9.
[10] G. Cheng, J.W. Zu, Two-frequency oscillation with combined Coulomb and viscous frictions, *American Society of Mechanical Engineers, Journal of Vibration and Acoustics* 124 (2002) 537–544.
[11] R.C. Hilborn, *Chaos and Nonlinear Dynamics*, Oxford University Press, Oxford, 1994.